Electronic-physical model that determines thermal conductivity of walls made of various materials

Aktam Denmukhammadiev*, *Abror* Pardaev, *Farrukh* Kucharov, and *Lobar* Nasimova

"Tashkent institute of irrigation and agricultural mechanization engineers", National Research University, Tashkent, Uzbekistan

Abstract. The article analyzes data on creating an electronic-physical model designed to determine the thermal conductivity of walls from various loose or solid materials used in the agricultural sector and construction. At the end of 2022 and the beginning of 2023, during the abnormally cold winter days observed in the Republic of Uzbekistan, accidents were observed at many construction sites and in heating networks. In response to this, by the government's decision, practical work was carried out to cover buildings' outer part (facade) with special basalt material. The studies of one-dimensional heat transfer in a compound cylinder carried out in a stationary mode at a constant thermal conductivity of the material, are analyzed. In these studies, heat conduction equations were studied with the results of heat transfer simulations developed using the Ansys software. The electronic-physical model proposed in the article allows you to quickly and accurately measure the heat and thermal diffusivity of walls made of various materials. It will be possible to intelligently control the electronic-physical model using thermal sensors. The article contains detailed engineering calculations and illustrative materials. Internet data was analyzed, and specific conclusions were drawn. The prerequisites for the creation of an intelligent system for measuring the temperature and thermal conductivity of walls from various bulk materials are made in the work.

1 Introduction

The analyzed work aims to study one-dimensional heat transfer in a compound cylinder. The study is carried out in a stationary mode at a constant thermal conductivity of the material. The heat equation is solved, and boundary and initial conditions are specified to obtain heat transfer simulation results developed using Ansys software. Dimensions, temperatures, and convective heat transfer coefficients are entered into Ansys to generate results. This software is used by engineers in all areas of physics, structural modeling, vibration, fluid dynamics, heat transfer, and electromagnetic interactions. This study mainly focuses on how a composite cylinder's temperature and heat flow change [1].

* Corresponding author: aquvvat@mail.ru

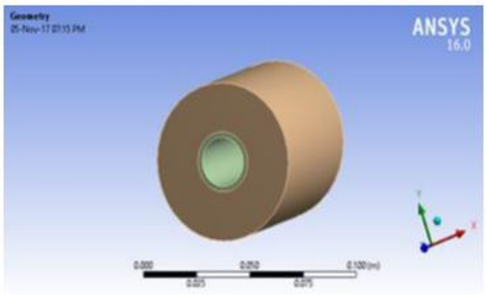

Fig.1. Analysis of cylinder in ANSYS [1].

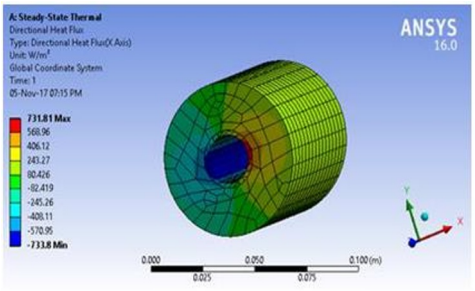

Fig.2. Variation of the cylinder's maximum and minimum directional heat fluxes [1].

As hot water flows through the middle of the cylinder, the highest temperature is observed. On the surface, as the cylinder was in contact with air, there the minimum temperature is noticed. As we move from the center of the cylinder towards the surface, the temperature decreases, as denoted in the above Figure 1 and Figure 2. The calculated minimum temperature of the cylinder is 58.255^0C, and the maximum temperature is 93.794^0C [1].

The heat transfer process through the building wall is complex and dynamic, which occurs through conduction, convection, and radiation[2]. For example, in the daytime, solar radiation hits the external wall surface, a part of which is released to the outdoor environment, and the other part is absorbed and conducted across the material. The interior surface of the wall then exchanges heat with the room air and other surfaces through convection and radiation. These heat transfer methods regulate the indoor air temperature and consequently influence the state of thermal comfort.

The heat exchange rate and direction through the building envelope depend on several parameters, including solar gain, indoor temperature, outdoor temperature, material thermophysical properties, and exposed surface area. The material thermophysical properties which affect the heat transfer rate are density, thermal conductivity, heat capacity, thermal resistance, thermal transmittance, and surface characteristics [3], [4]. Besides the thermophysical properties, material thickness affects the heat storage capacity of the wall as well [3], [4]. Also, the heat gain and loss through the wall can be influenced by the wall orientation and should be considered for energy-efficient building envelope design[5], [6]. The process of heat transfer through various walls has been studied [7], and illustrative materials are shown in Figure 3((a) and (b)).

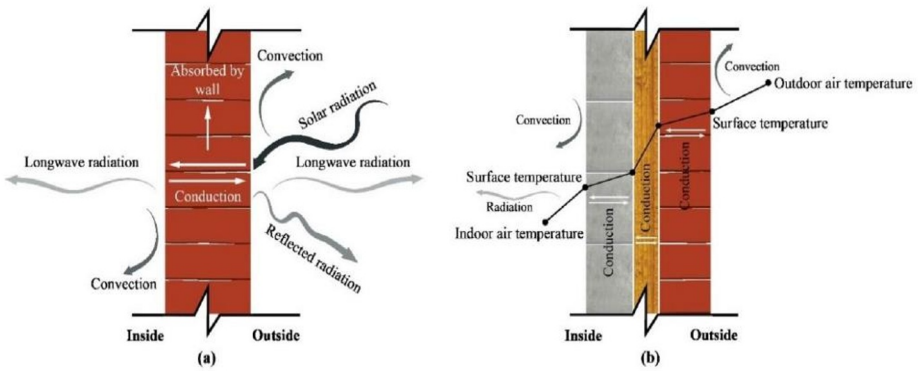

Fig. 3. Heat transfer process across (**a**) solid wall [8]; (**b**) composite wall.

Comparative Thermal Analysis of Walls Made of Traditional and Alternative Building Materials This study compares the thermal performance of walls made of building materials. Solving problems of this nature with the technology of heat processes requires using a special algorithm. An algorithm was developed and applied for this study. Using "Autodesk Inventor Professional 2020" and "Autodesk Inventor Nastran 2020", an algorithm for calculating the heat process was developed[8].

Classical in situ building wall thermal resistance measurements are based on steady-state assumptions. This limits their applicability, given their high sensitivity to outdoor conditions and the duration required to obtain accurate results. To overcome these limitations, the present paper introduces an in-situ method for assessing building wall thermal resistance. Dynamic (active) methodologies This section presents the two active methods developed. There are based on the same measurement data. The algorithms used were implemented in Matlab. To assess the repeatability and robustness of the method, several configurations were tested during the experimental campaign[9] (Figure 4).

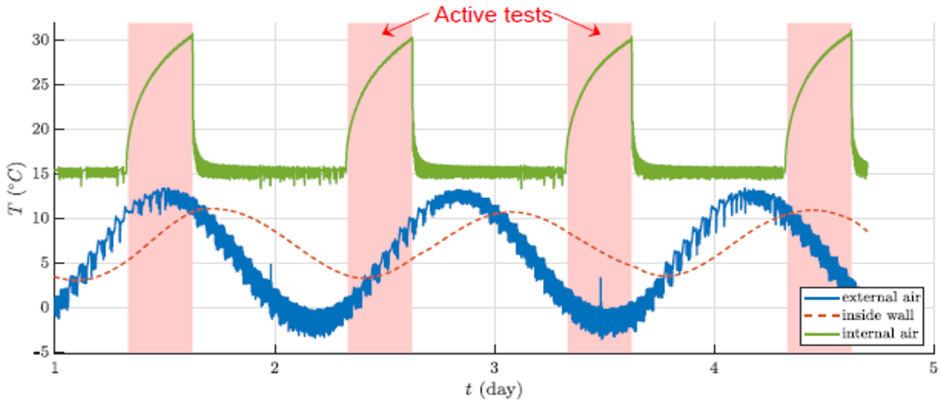

Fig.4: Example of internal and external temperatures for consecutive active tests (configuration 5) [10].

2 Methods

An analysis of the work [10] shows that the section "Heat transfer with a stationary thermal measurement method" describes the theoretical calculations for a stationary thermal measurement method in detail. It is also noted here that thermal energy transfer occurs simultaneously with thermal conductivity, convection, and radiation and that all three types of heat transfer are of interest for measurements. In the general case, in a linear system, the heat transfer process is usually written based on Newton's law in the form [11]

$$Q = \alpha \cdot F \cdot \Delta t \cdot \tau \qquad (1)$$

where Q is heat given (or received) by the body to the environment, J

F is heat exchange surface, m^2;

Δt is the driving force of the heat transfer process, which is the temperature difference between the body and the environment, deg;

τ is duration of the process, $\sec$;

α is heat transfer coefficient, $\frac{w}{m^2}$ deg.

In formula (1), we mean that it does not reflect the actual dependence of the heat flux on temperature, physical properties, and dimensions of the body and medium but is some formal technique, with the help of which all the difficulties of calculating heat transfer are transferred to determining the value of the coefficient α, which is less dependent on F and Δt than Q [11].

Therefore, the coefficient α is the summary heat transfer coefficient:

$$\alpha = \alpha_t + \alpha_k + \alpha_l \cdots \quad (2)$$

where α_t, α_k and α_l are heat transfer coefficients by conduction, convection, and radiation, respectively.

Heat transfer by thermal conduction occurs when there is a temperature gradient in the body, which is a physical factor that entirely determines the conditions for a heat flow. The relationship between the amount of heat Q transferred through the surface F during the time τ and the temperature gradient $\frac{\partial t}{\partial l} \cdot l$ is the basis of the Fourier law, the mathematical expression of which, taking into account the direction of the gradient (toward a higher temperature), has the form [11].

$$Q = \frac{\lambda}{l} \cdot F \cdot \tau \quad (3)$$

The coefficient of proportionality λ characterizes the body's ability to transfer thermal energy and is called the coefficient of thermal conductivity $\left(\frac{J}{m} \cdot \deg \cdot \sec\right)$.

In the process of thermal measurements, it is necessary to know the finite values of temperature differences, distances along the normal to the isothermal surface, and time intervals. Therefore, for the total amount of heat transferred through a flat wall during the time τ, the following expression is true:

$$Q = \frac{\lambda}{l} \cdot F \cdot (t_1 - t_2) \cdot \tau \quad (4)$$

Here l is wall thickness - the distance between the sections of the body in which the temperatures t_1 and t_2 are measured, m;

F is wall area through which the heat flux passes, m^2;

τ is time for which the heat flux is measured, sec.

Next value

$$q = \frac{Q}{F \cdot \tau} = \frac{\lambda}{l}(t_1 - t_2) \quad (5)$$

is called the specific heat flux or heat flux density. The ratio $\frac{\lambda}{l}$, by analogy with formula (1), can be called the heat transfer coefficient α_t by heat conduction.

When a solid body is in thermal contact with a liquid or gas flow, when there is a temperature difference between the body and the medium, a heat transfer process occurs called convective heat transfer. With this type of heat transfer, thermal energy is transferred by moving the material particles of the medium. In addition, convection can be accompanied by heat conduction.

Let us consider the similarity and differences between these processes in the examples of heat conduction through a three-layer wall (Fig. 5, a) and heat transfer through a flat wall, washed by flows from both sides (Fig. 5, (b)). For each layer (Fig. 5, (a)), one can write an equation for the temperature difference using the formula (5).

The result will be:

$$t_1 - t_4 = \left(\frac{l_1}{\lambda_1 F} + \frac{l_2}{\lambda_2 F} + \frac{l_3}{\lambda_3 F} \right) \frac{Q}{\tau} \qquad (6)$$

The brackets contain the sum of the thermal resistances of the individual layers.

During the convective exchange, the wall separates two media *A* and *B* (Figure 5(b)). In this case, we do not know the temperatures on the wall surfaces. Only the temperatures of the bulk of the liquids on both sides of the wall (t_1 and t_4) are known. In addition to the main mass of the liquid or core, boundary layers are formed near the wall during the flow of liquids. The concept of "boundary layer thickness" is rather arbitrary since there is no sharp transition from the boundary layer to the flow outside the layer. The following boundary layers are distinguished: hydrodynamic and thermal.

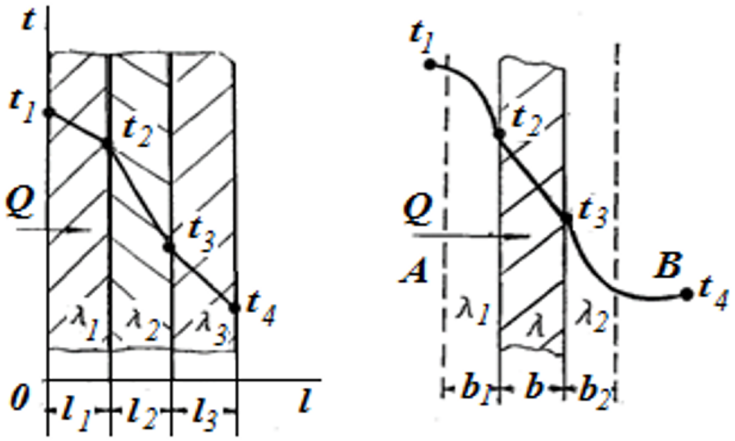

(a) *(b)*

Fig. 5. Heat transfer schemes [11]: (a) is through a multilayer flat wall; (b) is through a flat wall washed by streams on both sides.

The thickness of the hydrodynamic layer is understood as such a distance from the wall by which the velocity differs from the velocity of the undisturbed flow far away from the section by a certain value.

A thermal boundary layer is a layer of liquid or gas near the wall, within which the temperature changes from a value equal to the wall temperature to equal to the temperature of the liquid or gas away from the body, i.e., the entire change in the temperature of a liquid or gas (Figure 5, (b)) is concentrated in a relatively thin layer directly adjacent to the surface of the body.

The thickness of the boundary layer depends on many factors, particularly the physical and geometrical properties of the medium and its flow velocity.

In a linear approximation, the heat transfer through the boundary layer, by analogy with (4), can be represented for surface A as follows:

$$Q = \frac{\lambda_1}{b_1} F(t_1 - t_2)\tau = \alpha \cdot F \cdot \Delta t \cdot \tau \qquad (7)$$

where λ_1 is the coefficient of thermal conductivity of the medium; b_1 is the thickness of the wall area.

This means that the amount of heat transferred from the medium to the wall (or from the wall to the medium) could be easily determined, knowing the thickness of the boundary layer b_2. But such a possibility is ruled out. The fact is that the values b_1 and b_2 depend on many factors: the flow regime, the shape and roughness of the wall, the thermophysical properties of the flow, etc.[11].

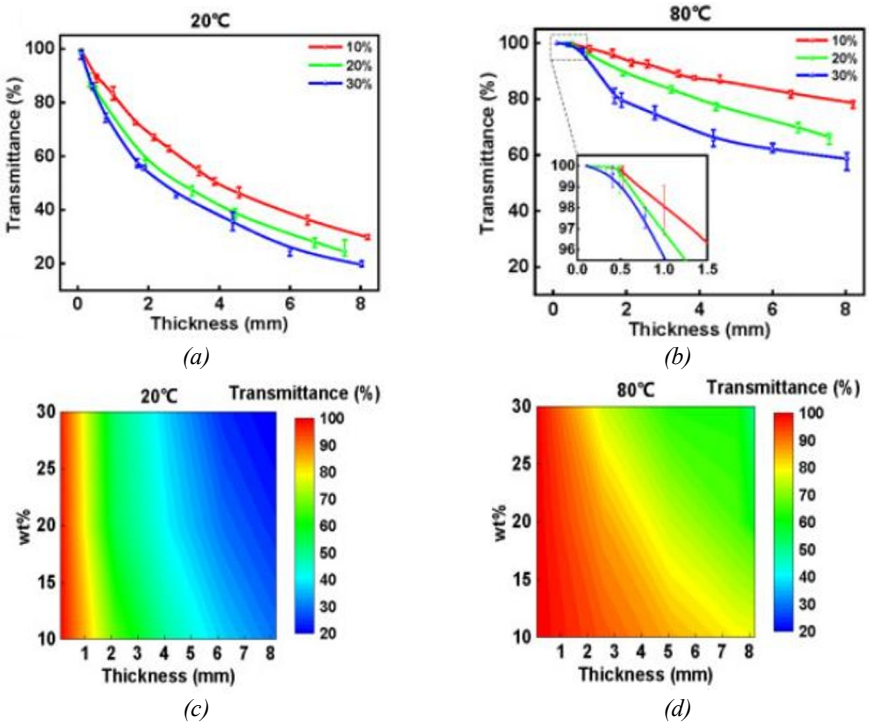

Fig. 6. Experimental data for transmission versus thickness of composites for different contents of paraffin in $20^0 C$ and $80^0 C$, respectively[12].

The article [12] analyzed modern methods for measuring body temperature with certain properties. As a result of studying the temperature-dependent thermal and mechanical properties of flexible, functional PDMS/paraffin composites, we reviewed materials and

methods, and the results of the thermal analysis show that the conductivity decreases with increasing wax amount and sample thickness. Compared to Figure 6 (a) and (b), it can be noted that the conductivity of the composites changed significantly after thermal treatment. When the composite sample was heated, the conductivity increased; when cooled, it decreased. The exchange between these two states was completely reversed. This switching phenomenon is well suited as a temperature measurement function of a flexible thermal control substrate. When the film's appearance changes from transparent milky white to transparent, the temperature rise of the substrate can be intuitively observed without temperature measurement equipment with a temperature change warning function. The contours in Figure 6 (c) and (d) illustrate the above conclusions more clearly[12].

We also studied materials for developing a new design of a thermal protection substrate for wearable electronics, capable of controlling heat flow and effectively absorbing thermal energy[13]. And in[14], the authors considered a heat-shielding substrate consisting of a functional soft composite, which includes an embedded phase material with a thin metal film over a soft polymer. According to the authors, a thermal underlay can significantly reduce peak skin temperature compared to a conventional underlay. It is also noted here that the thin copper foil and wax layer in the thermal barrier substrate can keep the substrate flexible, and the substrate loses its ability to stretch. This phenomenon limits the use of a heat-shielding substrate[15].

The electrical terminator uses a specially prepared smart thermometer. Several thermocouples have been tested in the laboratory for calibration. Table 1 lists their technical data. ThermoEMF depends not only on the temperature T_1 of the hot junction (that is, the measured temperature), but also on the temperature T_2 of the cold junction. The thermoEMF expression based on the Seebeck effect is given below [15]:

$$E = \alpha_1 \cdot (T_1 - T_2) \tag{8}$$

3 Results and Discussions

We have studied external and internal influences that adversely affect a multi-story building [16], the physical and mathematical models of seeds (as bulk material), and the errors in calculating the volume of the electroterminator filled with these seeds were studied [17] and a physical and electronic model of an infrared emitter for drying winding insulation was studied to create an intelligent heating control system and. winding insulation drying[18]. The intelligent system was also studied in the following work [19].

For many years we have been studying the electrophysical properties of crop seeds. Over the past 10 years, we have begun to closely engage in research on the study of the thermophysical properties of seeds; in particular, we have studied the thermal diffusivity and thermal conductivity of seeds as bulk materials. Below are some of the results of our research(Table 1,2 and Figure 7).

For different thermocouples, α_1 is value is given in Table 1.

Table 1. α_1 value for different thermocouples.

Serial number	**Type of thermocouple**	$\alpha_1, \left(\frac{mkV}{^0C}\right)$	**Working aisle** $\left(^0C\right)$
1	Copper-constantane	45	-150 to +350
2	Iron-constantan	53	-150 to +1000
3	Chromel-alumel	40	-200 to +500
4	Chromel-constantan	80	0 to +500
5	Platinum (platinum-rhodium)	6.3	0 to +1500

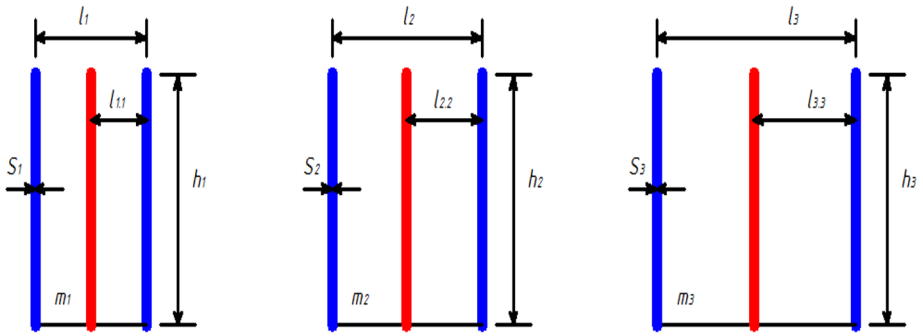

Fig. 7. Cross-sectional view of three types of cylindrical vessels (electroterminators)

In Figure 7, detailed information on the linear dimensions and weights of the vessels depicted in the figure is given in Table 1, the weight is given in grams, and the linear dimensions are given in millimeters.

Table 2. Research results

Vessel	**Weight**	**Height**	**Width**	**The distance between the electrodes**	**The thickness of the vessel wall**
Vessel-1	m_1 (gr)	h_1 (mm)	l_1 (mm)	$l_{1.1}$ (mm)	S_1 (mm)
	338	160	50.2	20.6	4.5
Vessel-2	m_{12} (gr)	h_2 (mm)	l_2 (mm)	$l_{2.2}$ (mm)	S_2 (mm)
	495	160	75.6	31.35	4.5
Vessel-3	m_1 (gr)	h_3 (mm)	l_3 (mm)	$l_{3.3}$ (mm)	S_3 (mm)
	844	160	108	49.3	4.5

For research, a cubic container with one open side was prepared(Figure 8, positions (a) and (b)), and its inner side was protected by a heat-insulating coating. Wall samples of different materials, with a surface exactly equal to the open side of the cube, were made in a square shape, the size corresponding to one side of the cube. In the closed bottom of the cube, in a special container (plate), pieces of ice were placed, and one open end of a thermocouple operating on the Seebeck effect was placed. The hot soldered end of the thermocouple was pressed against the inside of the square wall, and the other open end was attached to the thermocouple.

A special thermal chamber was used for the experiments. Inside the thermal chamber, more precisely, in the lower horizontal part of the thermal chamber, a cubic test container with a closed bottom was placed. The open side of the cube was sealed with a square wall taken for testing (thermocouples were left on the inside of the wall). The temperature inside the thermal chamber was maintained at the same level by the two-position heating method. In the above sequence, the temperature inside the thermal chamber (t_1) and the temperature inside the test wall cube (t_2) were determined, and engineering calculations were performed.

In order to reduce the error in the results of the experiment, the number of thermocouples was increased when measuring t_2 - temperature (for example, $t_{2.1}$, $t_{2.2}$, $t_{2.3}$ and $t_{2.4}$). The electrodes coming out of the thermocouples are connected to each other in parallel.

The results show that the measurement accuracy was greatest with 4 thermocouples.

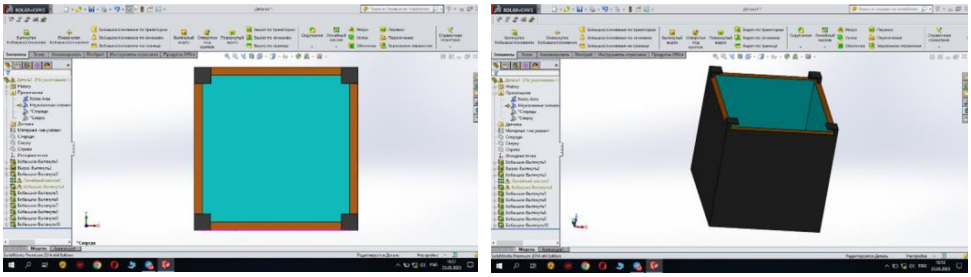

(a) *(b)*

Fig. 8. Cubic container with one open side: (a) view from above (b) side view

The temperature and the lamp were controlled by connecting the closed and open contacts of the magnetic starter using the time interval entered in the Delay Timer.

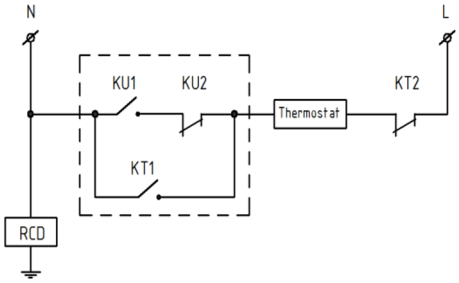

Fig. 9. Heating device control via thermostat

Fig. 10. Intelligent Temperature Control Sensor

To maintain the temperature at a given level, a thermostatic sensor tube is placed between the heating element. The required temperature for the study is set in the thermostat settings window(Figure 9). When the temperature reaches the set value, the RCD is disconnected from the network through the trip contact $KU2$ on the automation contactor. When registering readings below the adjusted temperature value, the connecting contacts $KT1$ turn on the heating element. The switches $KU1$ and $KU2$ of the RCD are,

respectively, on and off keys. In Figure 10**.** shows the display of an intelligent temperature control sensor used in laboratory experiments.

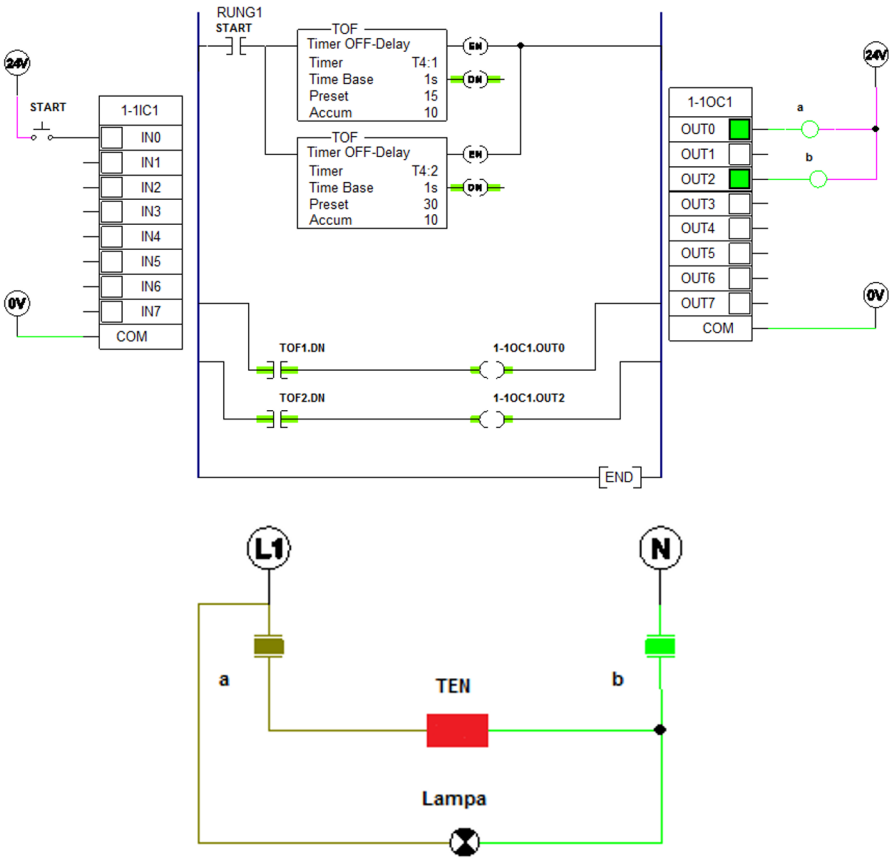

Fig. 11. Temperature and lamp control system in Automation Studio.

The temperature and lamp control model was developed using Automation Studio 5.2 software[20]. The running circuit was analyzed.

All components required for the circuit are selected from the main IEC electrical library. Variable(Figure 11) power supply $L1$ (Power Supply $L1$), neutral wire (Neutral), constant power supply $24V$ (Power Supply $24Volts$), normally open contact (Pushbutton Normally Open), normally Power on (Examine if Closed), lamp (Indicator Light), PLC input card (PLC Input Card), PLC output card (PLC Output Card), TEN (Electric toaster oven), magnetic starter coil (Coil), delay timer (Timer OFF-Delay). A temperature and lamp control model was developed based on the above components.

4 Conclusions

The prepared electronic-physical model makes it possible to measure the heat and thermal diffusivity of various types of wall samples with high accuracy. In this model, it will be possible to conduct high-precision express experiments throughout the year (in a state that

does not depend on the year's seasons). We have studied the intelligent systems used in construction and the agricultural sector and also made the prerequisites for creating an intelligent system for measuring the temperature and thermal conductivity of walls made of various bulk materials.

References

1. J. Jaivignesh *et al.*, Study of one dimensional conduction heat transfer for constant thermal conductivity through composite plane slab and in cylinder at steady state condition, *Int. J. Mech. Eng. Technol.*, vol. 8, no. 11, pp. 457–466, (2017).
2. B. Givoni, Man, climate and architecture, p. 483, Accessed: May 23, 2023. [Online]. Available: https://books.google.com/books/about/Man_Climate_and_Architecture. (1976)
3. S. Schiavoni, F. D'Alessandro, F. Bianchi, and F. Asdrubali, Insulation materials for the building sector: A review and comparative analysis, *Renew. Sustain. Energy Rev.*, vol. 62, pp. 988–1011, Sep., doi: 10.1016/J.RSER.2016.05.045(2016).
4. H. Asan, Numerical computation of time lags and decrement factors for different building materials, *Build. Environ.*, vol. 41, no. 5, pp. 615–620, doi: 10.1016/j.buildenv.2005.02.020(2006).
5. P. M. Toure, Y. Dieye, P. M. Gueye, M. Faye, V. Sambou, Influence of envelope thickness and solar absorptivity of a test cell on time lag and decrement factor, *J. Build. Phys.*, vol. 43, no. 4, pp. 338–350, Jan. 2020, doi: 10.1177/1744259119863446(2020).
6. F. Chi, Y. Wang, R. Wang, G. Li, C. Peng, An investigation of optimal window-to-wall ratio based on changes in building orientations for traditional dwellings, *Sol. Energy*, vol. 195, pp. 64–81, Jan., doi: 10.1016/J.SOLENER.2019.11.033(2020).
7. S. Yarramsetty, M. S. Rohullah, M. V. N. Sivakumar, and P. Anand Raj, An investigation on energy consumption in residential building with different orientation: a BIM approach, *Asian J. Civ. Eng.*, vol. 21, no. 2, pp. 253–266, Mar., doi: 10.1007/S42107-019-00189-Z(2020).
8. J. K. Nayak and J. A. Prajapati, Handbook on Energy Conscious Buildings, *R D Proj. no. 3/4(03)/99-SEC between Indian Inst. Technol. Bombay Sol. Energy Centre, Minist. Non-conventional Energy Sources*, vol. 4, no. 3, pp. 2093–2117, [Online]. Available: http://xlink.rsc.org/?DOI=C5EE01283J(2006)
9. R. Petkova-Slipets, K. Yordanov, and P. Zlateva, A comparative thermal analysis of walls composed of traditional and alternative building materials, *Civ. Environ. Eng.*, vol. 16, no. 2, pp. 388–395, Dec., doi: 10.2478/CEE-2020-0039(2020).
10. A. François, L. Ibos, V. Feuillet, J. Meulemans, "Estimation of the thermal resistance of a building wall with inverse techniques based on rapid active in situ measurements and white-box or ARX black-box models," *Energy Build.*, vol. 226, p. 110346, Nov., doi: 10.1016/J.ENBUILD.2020.110346(2020).
11. A.Azimov, P.Ismatullayev "Heat Exchange measuring trancducers. Publishing house "Fan" of the uzbek SSR, Tashkent, 76 p. (in Russian). (1974).
12. Y. Shi, M. Hu, Y. Xing, Y. Li, Temperature-dependent thermal and mechanical properties of flexible functional PDMS/paraffin composites, *Mater. Des.*, vol. 185, doi: 10.1016/j.matdes.2019.108219(2020).
13. Y. Shi, C. Wang, Y. Yin, Y. Li, Y. Xing, J. Song, Functional Soft Composites As Thermal Protecting Substrates for Wearable Electronics, *Adv. Funct. Mater.*, vol. 29, no. 45, Nov., doi: 10.1002/ADFM.201905470(2019).

14. N. Lu, S. Yang, Mechanics for stretchable sensors, *Curr. Opin. Solid State Mater. Sci.*, vol. 19, no. 3, pp. 149–159, doi: 10.1016/j.cossms.2014.12.007(2015).
15. B. Hoffschmidt, S. Alexopoulos, J. Göttsche, M. Sauerborn, O. Kaufhold, 3.06 - High Concentration Solar Collectors, *Compr. Renew. Energy*, pp. 165–209, Jan. 2012, doi: 10.1016/B978-0-08-087872-0.00306-1(2012).
16. A. Denmukhammadiev, A. Mustafoqulov, H. Valikhonova, E. Sobirov, T. Raimov, *Electricity metering and backup power supply for multi-storey buildings*, E3S Web Conf., vol. 264, pp. 1–9, doi: 10.1051/e3sconf/202126405051(2021).
17. A. Denmukhammadiev, A. Pardaev, M. Begmatov, I. Abdirakhmonov, M. Akhmedov, *Physicomathematical models of seeds and errors in calculating the volume of an electro terminator filled with seeds*, *E3S Web Conf.*, vol. 264, pp. 1–7, doi: 10.1051/e3sconf/202126401053(2021).
18. A. Denmukhammadiev, A. Pardaev, M. Begmatov, A. Mustafoqulov, H. Valikhonova, *Physical and electronic model of studying infrared radiator for drying wending insulation*, IOP Conf. Ser. Mater. Sci. Eng., vol. 1030, no. 1, doi: 10.1088/1757-899X/1030/1/012174(2021).
19. A. Djalilov *et al.*, *Intellectual system for water flow and water level control in water management*, IOP Conf. Ser. Earth Environ. Sci., vol. 614, no. 1, doi: 10.1088/1755-1315/614/1/012044(2020).
20. E. Edition, E7 e7 e7, p. 202(2020).